

Tailoring the waveforms to extend the high-order harmonic generation cut-off

I. A. Ivanov* and A. S. Kheifets

*Research School of Physical Sciences and Engineering,
The Australian National University, Canberra ACT 0200, Australia*

(Dated: May 30, 2019)

Abstract

Increase of the cut-off value in the high order harmonics generation process is demonstrated for a special case of the driving field composed of several harmonics of a given frequency. It is shown that a moderate, of the order of 20%, increase in the cut-off value can be achieved. This result possibly constitutes an upper limit for the increase in the cut-off value, attainable for a class of the waveforms considered in the paper.

* Corresponding author: Igor.Ivanov@anu.edu.au

I. INTRODUCTION

High order harmonic generation (HHG) is a nonlinear atomic process which can be described using a simple classical picture Corkum [1], Krause et al. [2], L'Huillier and Balcou [3]. Driven by a strong electromagnetic (EM) field, the atomic electron emerges into the continuum with zero velocity at some particular moment of time. At a later time, the classical electron trajectory returns to the nucleus, where the electron can recombine and emit a photon. The frequency of the emitted photon is determined by the amount of energy acquired by the electron and the atomic ionization potential (assuming that the electron recombines to the ground state). The classical analysis shows, that for the trajectories returning back to the nucleus, the electron kinetic energy cannot exceed the value of $3.17U_p$, where U_p is the ponderomotive potential. This leads to the well-known $I_p + 3.17U_p$ cut-off rule for the maximum harmonics order, which can be emitted in the recombination process.

The quantum counterpart of the classical model [4] assumes, that the released electron moves only under the action of the EM field neglecting the influence of the atomic potential (the so-called strong-field approximation - SFA). The SFA employs the analytical Volkov states, which makes the problem tractable. The classical returning trajectories emerge as extrema in the saddle-point analysis of the quantum-mechanical amplitudes computed within the SFA.

The aforementioned classical and quantum-mechanical results correspond to the pure cosine form of the driving EM field. Available pulse-shaping techniques [5] make it possible to modify the HHG characteristics by suitably tailoring the driving EM field. This problem belongs to a rapidly developing field of the quantum optimal control [6].

Several aspects of the optimal control of the HHG process were addressed in the literature. In the paper [7], the emission intensity of a given harmonic order was optimized by tailoring the laser pulse. In Ref. [8], the emphasis was placed on optimizing the particular high order harmonics from which single attosecond pulses could be synthesized. Both these works employed the so-called genetic algorithm, which mimicked the natural selection process by introducing the mutation procedure and suitable fitness function emphasizing the desired properties of the target state. Computationally, this procedure requires multiple solution

of the time-dependent Schrödinger equation (TDSE) which may constitute a considerable computational task if one is interested in formation of HHG in real atomic systems.

If the desired goal is to increase the harmonics cut-off order, there is a possibility to find the optimum field parameters using a purely classical approach based on the electron trajectory analysis [9]. The authors of this work tailored an ideal pulse shape providing an absolute maximum of the kinetic energy of the electron at the moment of its return to the nucleus. This energy was approximately 3 times larger than the corresponding energy for the pure cosine wave with the same period and field fluence. The waveform found in [9] was a linear ramp with the DC offset $F(t) = \alpha t + \beta$ for $t \in (0, T)$, T being the period of oscillations. To avoid using a strong DC field in practice, it was suggested in [9], that it could be replaced by an AC field of a lesser $\Omega/2$ frequency, while the linear ramp could be replaced by a combination of the harmonics with frequencies $n\Omega$. Here Ω is the frequency corresponding to the oscillation period T , n is integer. The overall pulse has thus a period of $2T$, rather than T . The weights corresponding to different harmonics constituting the pulse were found by means of the genetic algorithm. Results of the quantum calculation relying on SFA reported in [9] confirmed, that this waveform allowed to achieve considerable increase in the cut-off position without drop of intensity. That waveform containing component with the halved frequency $\Omega/2$ leads to the considerable increase in the cut-off position is perhaps not surprising, given that ponderomotive energy grows as $1/\Omega^2$. An important point is that for this waveform the increase in the cut-off position is not accompanied by the drop of intensity.

In the present work, we address a related question: what gain in the HHG cut-off can be achieved if we use the driving EM field with the waveform composed of the harmonics with the multiple frequencies $n\Omega$. In other word, we demand the driving EM pulse to be strictly T -periodic and such, that its integral over a period is zero (i.e., no DC component is present). It turns out, that a moderate increase in the cut-off position is possible in this case. A simpler case of adding the second harmonic 2Ω to the waveform was considered in earlier works [10, 11]

We supplement the classical trajectory analysis by a quantum mechanical TDSE cal-

culuation of the HHG process in the lithium atom. Numerical solution of TDSE takes full account of the effect of the atomic potential. Such a calculation ensures, that the effect of the extended HHG cut-off, which we report below, is not an artifact of a simplified treatment.

II. THEORY

A. Classical approach

We begin with a purely classical problem of finding returning trajectories of an electron moving in a periodic EM field with a given period T , corresponding frequency $\Omega = 2\pi/T$, and which does not contain DC component:

$$F(t) = 2\text{Re} \sum_{k=1}^K a_k e^{ik\Omega t} \quad (1)$$

Our task is to find the set of coefficients a_k in Eq. (1) for which electron returning to the nucleus possesses the highest possible kinetic energy. For this problem to be well-defined, we must impose some restrictions on the possible choice of this set. A natural requirement is that only the fields $F(t)$ with the fixed fluency are to be considered. This implies that $4 \sum_{k=1}^K |a_k|^2 = F_0^2$, where the field strength F_0 is related to the intensity via $I = 3.5 \times 10^{16} F_0^2$. Here the field intensity is measured in W/cm² and the field strength is expressed in the atomic units.

As it is customarily done in the classical 3-step model of HHG, we neglect the influence of the atomic core on the electron motion. We solve the classical equations of motion of an electron in the EM field given by Eq. (1) with the initial conditions $x(t_0)=0$, $\dot{x}(t_0) = 0$. Here t_0 is the moment of time when atomic ionization event occurs. We are interested only in the returning trajectories for which $x(t_1)=0$ for some t_1 . For such trajectories, we compute the kinetic energy E at the moment of return.

We use the following field parameters: $I = 10^{12}$ W/cm², $F_0 = 0.0053$ a.u., $\Omega = 0.185$ eV. In this and the subsequent section we consider the case of the Li atom with the ionization potential $I = 0.196$ a.u. For this set of the field and atomic parameters, the value of the Keldych parameter $\gamma = \sqrt{I_p/2U_p}=0.8$

For the pure cosine form of the EM field, this procedure leads to the typical dependence of the kinetic energy at the moment of return on the time of release shown in Figure 1 by the solid (red) line. For convenience, in Figure 1 we plot not just the kinetic energy itself, but the quantity $N = (E + I_p)/\Omega$, which gives us a number of photons emitted in the recombination process. The solid curve in Figure 1 shows that, for the parameters we chose, the maximum number of emitted photons is approximately $N_{\text{cut-off}} \approx 100$, which is a visualization of the well-known $I_p + 3.17U_p$ cut-off rule.

For the set of parameters in Eq. (1), defining the EM field different from the pure cosine wave, we proceed as follows. We start with the pure cosine wave and maximize the kinetic energy E of the returning electrons by performing a directed search in the space of the coefficients a_k . As was noted above, the constraint of the fixed fluency is imposed such that the fluency had the same value as in the case of the pure cosine wave we considered above.

We perform two calculations of this kind. In the first, we impose an additional restriction that only the terms with odd k -values are to be present in Eq. (1). This ensures that the resulting HHG spectrum contains only odd harmonics of the main frequency. In the second calculation, we retain the terms with both odd and even k -values in the expansion (1). The first calculation was performed with $K = 7$, while in the second we chose $K = 5$. The resulting sets of coefficients a_k for which the maximum of the highest kinetic energy of the returning electron is attained, are presented in Table I. Also presented is the set consisting of only a_1 , which defines the pure cosine wave for the field parameters considered above.

The degree to which this procedure increases the highest energy of the returning electron is illustrated in Figure 1. Resulting shapes of the driving field $F(t)$, corresponding to the three cases considered above are visualized in Figure 2.

As one can see, the set of the parameters corresponding to only odd harmonics present in Eq. (1) allows to achieve a 10% gain in the position of the cut-off. The curve representing dependence of the kinetic energy on the time of release remains symmetric with respect to the translation $t \rightarrow t + T/2$, as in the case of the pure cosine wave. This is, in fact, a general property exhibited by the classical solutions of the equations of motion in the EM field with only odd harmonics present in Eq. (1), which leads to essentially the same structure of the

	cosine wave	odd harmonics	odd and even harmonics
k	$a_k \cdot 10^3$	$a_{2k-1} \cdot 10^3$	$a_k \cdot 10^3$
1	2.665	$2.503 - 0.076i$	$2.123 - 1.033i$
2	0	$-0.443 - 0.566i$	$0.403 + 0.754i$
3	0	$0.061 - 0.385i$	$-0.558 + 0.271i$
4	0	$0.138 - 0.264i$	$-0.302 - 0.358i$
5	0	0	$0.224 - 0.248i$

TABLE I: Coefficients in Eq. (1) for which the highest kinetic energy of the returning electron is maximized. The second column: pure cosine wave; the third column: odd harmonics with $K = 7$; the fourth column: odd and even harmonics with $K = 5$

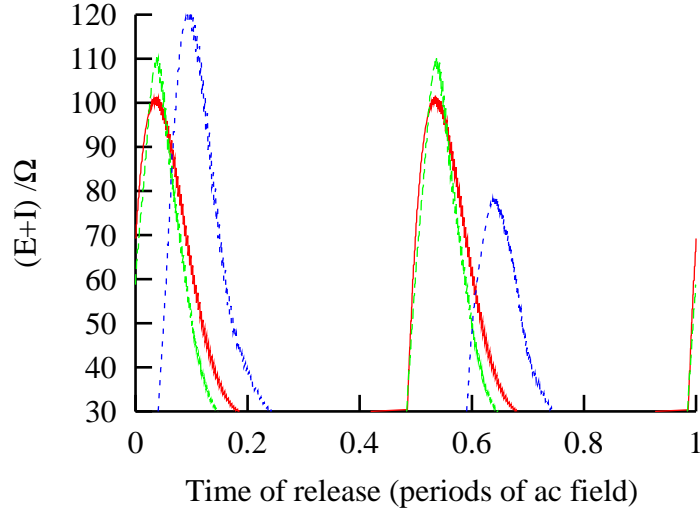


FIG. 1: (Color online) Classical dependence of the quantity $(E + I_P)/\Omega$ on the time of electron release within an optical cycle (E - electron energy at the moment of return to the nucleus, $I_P = 0.196$ a.u.- ionization potential of the Li atom). The three sets of curves correspond, respectively, to the pure cosine wave – solid (red) line; odd harmonics in Table I – dashed (green) line; odd and even harmonics in Table I – short (blue) dash.

classical returning electron trajectories as in the case of the cosine wave. There are two such trajectories per every half cycle of the EM field (the so-called "long" and "short" trajectories) for the plateau region, i.e. for the kinetic energies below the apex of the corresponding

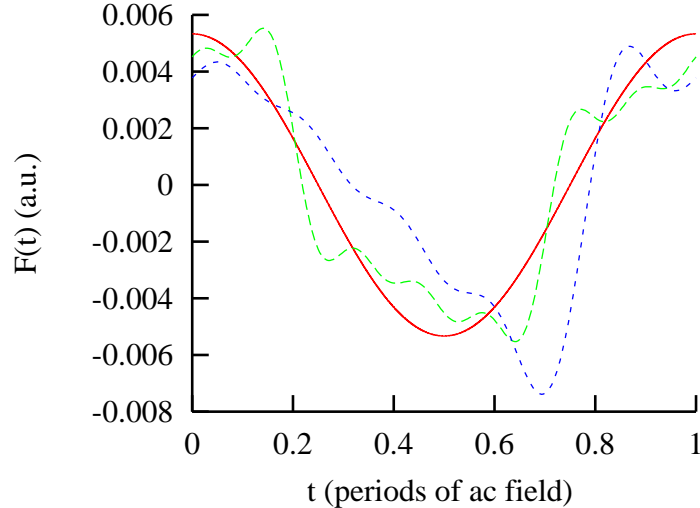


FIG. 2: (Color online) EM fields corresponding to the coefficients a_k listed in Table I. The pure cosine wave – (red) solid line; odd harmonics in Eq. (1) with $K = 7$ – (green) dashed line; odd and even harmonics in Eq. (1) with $K = 5$ – (blue) short dash.

curves in Figure 1. There is one trajectory per every half cycle with the kinetic energy of the returning electron near the apex of the curves (the cut-off harmonics).

Situation is different for the case of even and odd harmonics present in the Eq. (1). The kinetic energy curves are no longer symmetric with respect to the half cycle translation $t \rightarrow t + T/2$.

One should note, that increase in the cut-off position shows very little sensitivity to further increase of the number of terms in Eq. (1). If, for example, we used $K = 9$ instead of $K = 7$ in the case of only odd harmonics included in Eq. (1), we would have gained additional increase in the cut-off position of the order of 1%. Similar observation applies for the case of even and odd harmonics in Eq. (1). This indicates, that the low order harmonics in the series (1) are primarily responsible for the increase in the cut-off position, and the pulses composed using the coefficients in Table I are optimal in the sense that no further significant increase in the cut-off position is possible as long as we rely on the expansion (1) for the waveform.

The discussion presented so far was purely classical and constituted a simple generalization of the 3-step model for the case of the EM field given by Eq. (1). Quantum calculation

is needed to confirm the classical results. Such calculation is presented in the next section.

B. Quantum calculation

In this section, we present results of the HHG calculation for the Li atom for the set of coefficients a_k given in Table I. We use the procedure, which we developed recently in Ref. [12] for the solution of TDSE for realistic atomic targets, which can be described within the single active electron approximation. For completeness, most essential features of this procedure are outlined below.

The field-free atom in the ground state is described by solving a set of self-consistent Hartree-Fock equations [13]. The field-free Hamiltonian \hat{H}_{atom} in this model is thus a non-local integro-differential operator.

The EM field is chosen to be linearly polarized along the z -axis. We describe the atom-EM field interaction using the length gauge: $\hat{H}_{\text{int}} = zF_z(t)$, where $F_z(t) = f(t)F(t)$. Function $F(t)$ is given by Eq. (1) where we use one of the three sets of the coefficients from Table I. The switching function $f(t)$ smoothly grows from 0 to 1 on a switching interval $0 < t < T_1$, and is constant for $t > T_1$. The switching time is $T_1 = 5T$.

We represent solution of TDSE in the form of an expansion on a set of the so-called pseudostates:

$$\Psi(\mathbf{r}, t) = \sum_j b_j(t) f_j(\mathbf{r}) \quad (2)$$

This set is obtained by diagonalizing the field-free atomic Hamiltonian on a suitable square integrable basis [14, 15]:

$$\langle f_i^N | \hat{H}_{\text{atom}} | f_j^N \rangle = E_i \delta_{ij} . \quad (3)$$

Here the index j comprises the principal n and orbital l quantum numbers, E_j is the energy of a pseudostate and N is the size of the basis.

To construct the set of pseudostates satisfying Eq. (3), we use either the Laguerre basis, or the set of B-splines (for angular momenta $l > 15$), confined to a box of a size $R_{\text{max}} = 200$ a.u. B-splines of the order $k = 7$ with the knots located at the sequence of points lying in $[0, R_{\text{max}}]$ are employed. All the knots t_i are simple, except for the knots located at the origin

and the outer boundary $R = R_{\max}$ of the box. These knots have multiplicity $k = 7$. The simple knots were distributed in $(0, R_{\max})$ according to the rule $t_{i+1} = \alpha t_i + \beta$. The parameter α was close to 1, so that the resulting distribution of the knots was almost equidistant. For each value of the angular momentum l , the first $l+1$ B-splines and the last B-spline resulting from this sequence of knots were discarded. Any B-spline in the set thus decreases at least as fast as r^{l+1} and assumes zero value at the outer boundary.

In the present calculation, the system is confined within a box of a finite size which may lead to appearance of spurious harmonics in the spectrum due to the reflection of the wavepackets from the boundaries of the box [2]. One can minimize this effect by using a mask function or an absorbing potential. We use the absorbing potential $-iW(\mathbf{r})$ which is a smooth function, zero for $r \leq 180$ a.u. and continuously growing to a constant $-iW_0$ with $W_0 = 2$ a.u. outside this region.

For the EM field parameters which we employed in the classical treatment of the previous section, the maximum number of photons emitted in the recombination process is of the order of a hundred. This implies that to describe accurately formation of all harmonics, we have to retain pseudostates with correspondingly high angular momenta. In the calculation we present below, the pseudostates with angular momenta $l < 120$ were retained in Eq. (2).

With the total Hamiltonian and basis set thus defined, the TDSE can be rewritten as a system of differential equations for the coefficients $b_j(t)$ in 2. This system is solved for the time interval $(0, 30T)$, where T is a cycle of the AC field, using the Crank-Nicholson method [16].

Finally, the harmonics spectrum is computed as [2]:

$$|d(\omega)|^2 = \left| \frac{1}{t_2 - t_1} \int_{t_1}^{t_2} e^{-i\omega t} d(t) dt \right|^2. \quad (4)$$

Here $d(t) = \langle \Psi(t) | z | \Psi(t) \rangle$ is expectation value of the dipole momentum, limits of integration t_1 and t_2 are chosen to be large enough to minimize the transient effects (we use last 10 cycles of the pulse duration, i.e., $t_1 = 20T$, $t_2 = 30T$).

III. RESULTS

In Figure 3 we show the harmonics spectra resulting from the TDSE calculation for the three choices of the EM field coefficients listed in Table I. We remind the reader that in all three cases fluencies are equal, corresponding to the same field intensity $I = 10^{12}$ W/cm².

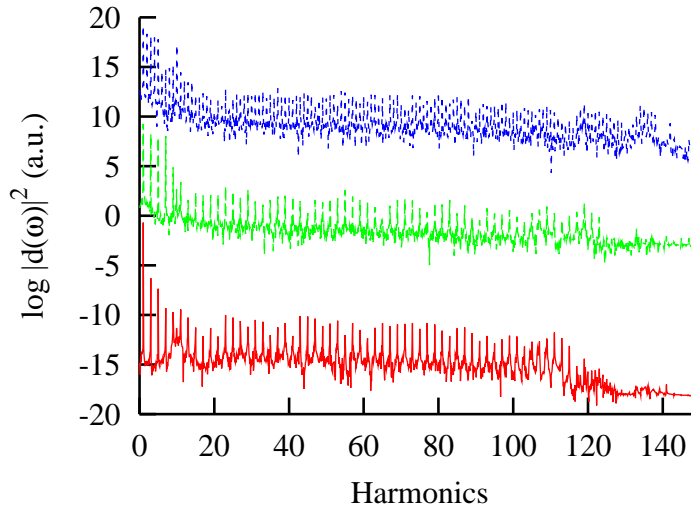


FIG. 3: (Color online) Harmonics spectra of Li for the EM fields from Table I. Pure cosine wave ((red) solid line); odd harmonics in Eq. (1) with $K = 7$ (green) dashed line, for convenience of comparison the quantity $\log |d(\omega)|^2 + 10$ is shown; odd and even harmonics in Eq. (1) with $K = 5$ (blue) short dash, the quantity $\log |d(\omega)|^2 + 20$ is shown.

General appearance of these spectra agrees with the expectations based on the classical results of the previous section. One can observe the increase in the cut-off position for the pulse shaped according to the recipe from the third column of Table I (only odd harmonics with $K = 7$ in Eq. (1)), comparing to the cut-off position for a pure cosine wave of the same fluency. Cut-off position increases yet further for the pulse constructed using the set of the coefficients from the fourth column of Table I (odd and even harmonics with $K = 5$ in Eq. (1)). In this case, the spectrum contains harmonics of both odd and even orders. A magnified fragment of the spectrum illustrating this fact is shown in Figure 4. As can be observed from Figure 3, an increase in the cut-off position occurs without any drop of the harmonics yield.

Quantitatively, the TDSE results for the cut-off positions are in good agreement with

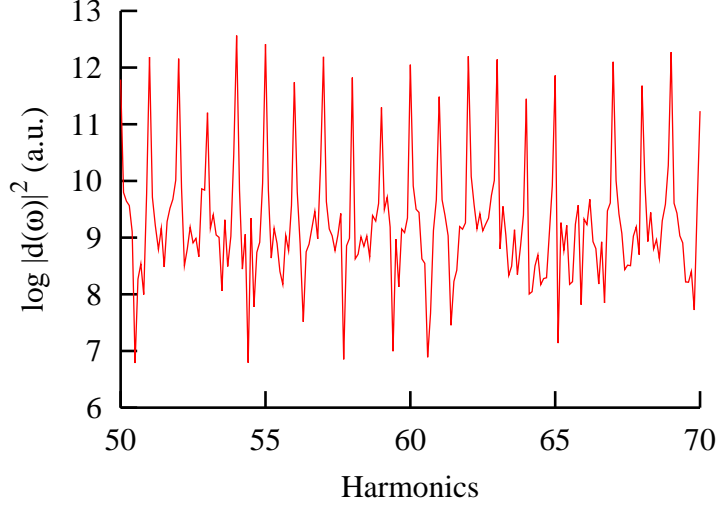


FIG. 4: (Color online) Part of the spectrum of Li for odd and even harmonics in Eq. (1) with $K = 5$.

the classical predictions, summarized in Figure 1. Use of the pulse constructed from all harmonics with $K = 5$ in Eq. (1) allows to increase the cut-off position by about 20%, in agreement with the classical analysis given above.

We can, in fact, establish a closer correspondence between classical and quantum results by performing the time-frequency analysis of our data. The techniques used for this purpose, the wavelet transform [7, 17, 18, 19], or the closely related Gabor transform [17, 20], offer possibility to track the process of harmonics formation in time, combining both the frequency and temporal resolution of a signal. By using these techniques, we can try to find, in the quantum domain, the traces left by the classical trajectories. The fact that such traces may be present, follows from the quantum-mechanical treatment of the HHG process given in [4], where the classical trajectories naturally appear in the saddle-point analysis. Such manifestation of the classical trajectories in the HHG spectra was demonstrated, for example, for the hydrogen atom [19].

We perform our analysis of the HHG process by applying the wavelet transform of the dipole operator $d(t)$ in Eq. (4). This transform is defined as [21]

$$T_{\Psi}(\omega, \tau) = \int d(t) \sqrt{|\omega|} \Psi^*(\omega t - \omega \tau) dt . \quad (5)$$

The transform is generated by the Morlet wavelet $\Psi(x) = x_0^{-1} \exp(-ix) \exp[-x^2/(2x_0^2)]$.

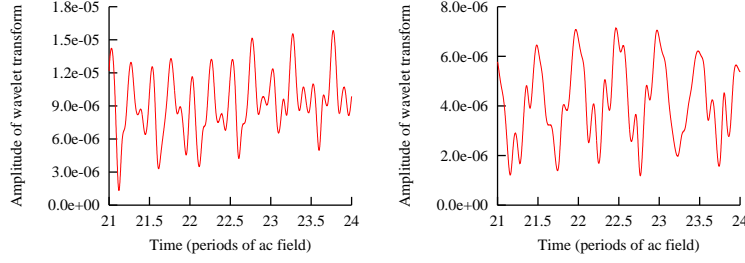


FIG. 5: (Color online) Wavelet time-spectrum of Li for the 61-st (left panel) and 101-st (right panel) harmonics for the pure cosine wave in Eq. (1).

Figure 5 presents a well-known picture of the harmonics formation in time [19]. For the plateau harmonics, the amplitude of the wavelet transform has four maxima per cycle, corresponding to the two pairs of the so-called long and short trajectories for the harmonics at the plateau. For the near cut-off 101-st harmonic, two maxima per cycle are present. Those features agree completely with the classical picture shown in Figure 1.

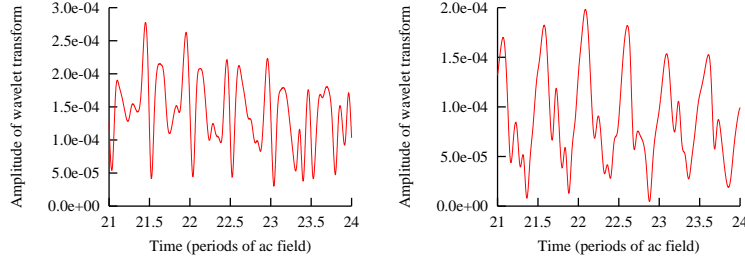


FIG. 6: (Color online) Wavelet time-spectrum of Li for the 65-th (left panel) and 99-th (right panel) harmonics for the pulse with only odd harmonics in Eq. (1) ($K = 7$).

For the pulse containing only odd harmonics in Eq. (1), classical picture of the dependence of kinetic energy on the time of release, presented on Figure 1, is very similar to the curve for the pure cosine wave. We can expect, therefore, results of the wavelet transform in this case to be qualitatively similar to those shown on Figure 5. That this is indeed the case can be observed from the Figure 6.

For the field waveform containing both odd and even harmonics in Eq. (1), the classical analysis reveals a somewhat different picture. As one can see from Figure 1, there are two pairs of the classical trajectories per cycle for which kinetic energy of the returning

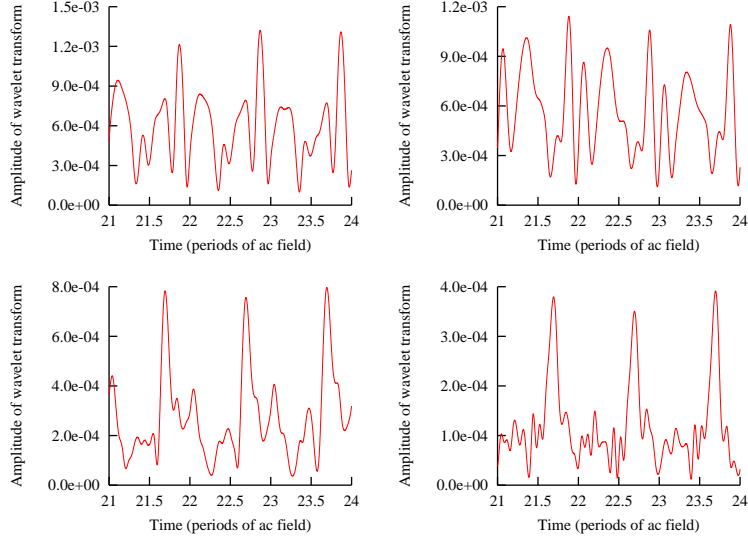


FIG. 7: (Color online) Wavelet time-spectrum of Li for the 65-th, 75-th, 97-th and 111-th harmonics (from left to right and top to bottom). The driving field contains terms with both odd and even k -values in Eq. (1) with $K = 5$.

electron is such, that less than approximately 60 photons are emitted upon recombination. When the number of emitted photons increases and reaches the value of approximately 75 (cut-off region for the smaller maximum of the corresponding curve in Figure 1), there are three returning trajectories per cycle. For higher energies, there remain only two classical trajectories, which can participate in the formation of the harmonics. For higher yet energy, a single such trajectory exists.

As can be observed from Figure 7, the quantum calculation apparently confirms these classical considerations. Wavelet spectra do demonstrate that number of maxima per cycle progressively decreases with the increase of the harmonics order.

IV. CONCLUSION

We demonstrated an increase of the cut-off value for the HHG process when a superposition of several harmonics of a given frequency is used to build a wavefront of the driving EM field. We analyzed the classical returning electron trajectories for the fields thus constructed. Such an analysis shows, that a field spectral composition can be found, for which a 20%

increase in the value of the maximum classical kinetic energy of the recombining electron is achieved as compared to the case of a cosine wave of the same fluency.

TDSE calculation of the HHG spectrum for such a driving field, performed for the Li atom, confirms the classical result. It does demonstrate the increase in the cut-off value of the order of 20% without any drop of the harmonics intensity. This value represents a maximum increase which can be achieved if we restrict the trial waveform to that given by Eq. (1) under condition of a fixed fluency. Indeed, the classical calculation shows, that no further noticeable increase of the maximum classical kinetic energy of the recombining electron can be achieved by adding higher order harmonic terms in expansion (1).

Our result thus presents an upper limit in the increase of the HHG cutoff achieved for the class of the waveforms given by Eq. (1), i.e. for the waveforms which are periodic with a given period T and do not contain the DC components. This suggests, that to achieve more substantial increase in the HHG cutoff condition, one should use the waveforms which cannot be described by Eq. (1). Such are the ideal waveform proposed in [9], for which we should allow the term with $k = 0$ to the sum in Eq. (1)), or the field configurations containing subharmonic fields with frequencies $\Omega/2$, as those used in [9, 22]. As results of these works indicate, a considerably more important gain in the cutoff energy can be achieved for such waveforms. These results, and the result obtained in the present work, allow us to draw the following conclusion. The strategy based on the low-frequency (subharmonic) modifications of the waveform may be more efficient than the strategy relying on introducing multiple-frequency components in the trial waveform as in Eq. (1). This may provide a useful guide to the problems related to modification of the high frequency part of the HHG spectrum.

The time-frequency analysis of the results of the TDSE calculation illustrates the role, which the classical trajectories play in the formation of the harmonics. The usual picture of HHG rendered by this technique exhibits traces of four (for the plateau harmonics) or two (harmonics near cut-off) trajectories per optical cycle, which participate in forming a particular harmonic. In the case of the waveform constructed from the terms of odd and even order in Eq. (1), the picture revealed by the wavelet analysis is different. Number of contributing trajectories in this case varies with energy in agreement with the classical

picture of Figure 1. Depending on the harmonics order, there may be four, three, two or just a single such trajectory.

V. ACKNOWLEDGEMENTS

The authors acknowledge support of the Australian Research Council in the form of the Discovery grant DP0771312. Resources of the National Computational Infrastructure (NCI) Facility were employed. One of the authors (ASK) wishes to thank the Kavli Institute for Theoretical Physics for hospitality. This work was supported in part by the NSF Grant No. PHY05-51164

References

-
- [1] P. B. Corkum, Phys. Rev. Lett. **71**, 1994 (1993).
 - [2] J. L. Krause, K. J. Schafer, and K. C. Kulander, Phys. Rev. A **45**, 4998 (1992).
 - [3] A. L’Huillier and P. Balcou, Phys. Rev. Lett. **70**, 774 (1993).
 - [4] M. Lewenstein, P. Balcou, M. Y. Ivanov, A. L’Huillier, and P. B. Corkum, Phys. Rev. A **49**, 2117 (1994).
 - [5] A. M. Weiner, D. E. Leaird, J. S. Patel, and J. R. Wullert, IEEE J. Quantum Electron. **28**, 908 (1992).
 - [6] J. Werschnik and E. K. U. Gross, J. Phys. B **40**, R175 (2007).
 - [7] X. Chu and Shih-I Chu, Phys. Rev. A **64**, 021403(R) (2001).
 - [8] A. B. Yedder, C. Le Bris, O. Atabek, S. Chelkowski, and A. D. Bandrauk, Phys. Rev. A **69**, 041802(R) (2004).
 - [9] L. E. Chipperfield, J. S. Robinson, J. W. G. Tisch, and J. P. Marangos, Phys. Rev. Lett. **102**, 063003 (2009), URL <http://link.aps.org/abstract/PRL/v102/e063003>.
 - [10] J. Mauritsson, P. Johnsson, E. Gustafsson, A. L’Huillier, K. J. Schafer, and M. B. Gaarde, Physical Review Letters **97**, 013001 (pages 4) (2006), URL <http://link.aps.org/abstract/PRL/v97/e013001>.

- [11] Z. Zeng, Y. Cheng, X. Song, R. Li, and Z. Xu, Physical Review Letters **98**, 203901 (pages 4) (2007), URL <http://link.aps.org/abstract/PRL/v98/e203901>.
- [12] I. A. Ivanov and A. S. Kheifets, J. Phys. B **41**, 115603 (2008).
- [13] L. V. Chernysheva, N. A. Cherepkov, and V. Radojevic, Comp. Phys. Comm. **11**, 57 (1976).
- [14] I. Bray, Phys. Rev. A **49**, 1066 (1994).
- [15] I. Bray and A. T. Stelbovics, Adv. Atom. Mol. Phys. **35**, 209 (1995).
- [16] A. Goldberg, H. M. Schey, and J. L. Schwartz, Am. J. Phys. **35**, 177 (1967).
- [17] P. Antoine, B. Piraux, and A. Maquet, Phys. Rev. A **51**, R1750 (1995).
- [18] X. M. Tong and Shih-I Chu, J. Phys. B **32**, 5593 (1999).
- [19] X. M. Tong and Shih-I Chu, Phys. Rev. A **61**, 021802(R) (2000).
- [20] R. Taïeb, V. Vénierd, J. Wassaf, and A. Maquet, Phys. Rev. A **68**, 033403 (2003).
- [21] Y. Y. Tang, L. H. Yang, J. Liu, and H. Ma, *Wavelet Theory and Its Application to Pattern Recognition* (World Scientific, 2000).
- [22] T. Pfeifer, L. Gallmann, M. J. Abel, P. M. Nagel, D. M. Neumark, and S. R. Leone, Physical Review Letters **97**, 163901 (pages 4) (2006), URL <http://link.aps.org/abstract/PRL/v97/e163901>.